

Pipeflow downstream of a reducer and its effects on flowmeters

T. T. Yeh and G. E. Mattingly

Fluid Flow Group, Process Measurements Division, Chemical Science and Technology Laboratory, National Institute of Standards and Technology, Gaithersburg, MD 20899, USA

Received 1 December 1993

The pipeflow profile and its influence on orifice coefficients downstream of a reducer have been studied experimentally in a 5.25 cm (2.07 in) diameter water flow facility. The mean and turbulence velocities, obtained by laser Doppler velocimetry (LDV) are presented. From the measured velocity profiles, the profile characteristics of the pipeflow are described qualitatively and quantitatively. Several profile indexes are introduced to characterize the profile features (peaknesses and flow displacements). These indexes are then correlated with flowmeter performance in these flows. It is shown that these profile indexes correlate well with changes in discharge coefficient for the orifice meters and thus could be used to develop criteria for improving the performance of orifice meters or other types of meter in non-ideal installation conditions.

Keywords: orifice meters; pipeflow profile; laser Doppler velocimetry

Introduction

This paper presents results obtained in an industry-government consortium-sponsored research program on flowmeter installation effects being conducted at NIST-Gaithersburg, MD. The program is a cooperative research effort on generic technical issues to produce flow metering improvements needed by industry when meters are installed in non-ideal conditions. Ideal meter installation conditions are those where long straight lengths of constant diameter piping precede the meter locations. Actual installations seldom conform to these conditions. The non-ideal condition is any of the infinitude of conditions where the upstream piping conditions produce pipeflow distributions that differ from those associated with fully developed flow. These non-ideal pipeflows can significantly affect the flowmeter performance.

Improvements for meter performance are sought from many starting points. Normally, meters are retrofitted into fluid systems that were not designed for them and are thus installed and operated in non-ideal installation conditions. Flow metering improvements are also desired for existing meter systems – either by upgrading the inlet flow conditions or by replacing the metering device itself so that accuracy levels are increased. Flow conditioning devices of one geometry or another are frequently recommended for improving flowmeter performance when installation conditions are not ideal: however, it has been shown that certain flow conditioner installations can produce serious

deviations from the ideal installation performance of specific meters. To establish accurate flowmeter performance in the flows produced by different pipe configurations, we would have to understand the basic flow fields involved and how these interact with the specific meter geometry.

The objective of the NIST research program is (a) to produce a basic understanding of the flow phenomena that are produced in non-ideal pipe flows and to quantify these phenomena relative to reference fluid dynamic conditions; and (b) to correlate meter-factor shifts for flowmeters installed downstream from these pipeline elements with quantified flow features so as to be able to improve meter performance in non-ideal installations. The program is based upon measurements of pipeflows using laser Doppler velocimetry (LDV) and meter calibrations using transfer standards. This approach has been utilized in several different types of flowmeter installations downstream of several different pipe configurations.¹⁻⁵ These results have also been incorporated into the new standards on methods for establishing flowmeter installation effects.⁶

The pipeflow produced by conventional concentric reducers is the focus of the present experimental study. The piping configuration is sketched in Figure 1 with the coordinate system selected. The results given are the velocity profile measurements and the performance characteristics of a range of orifice meter geometries downstream of the reducer.

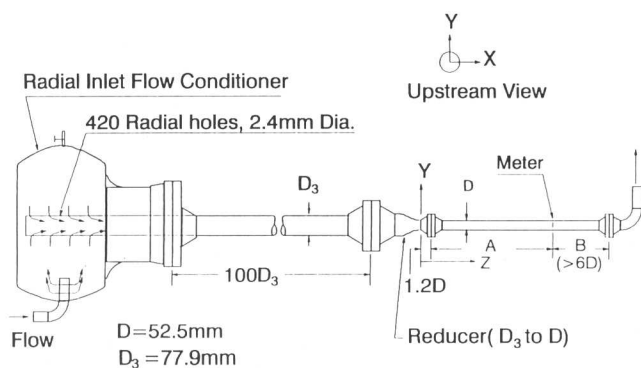


Figure 1 Sketch of the reducer piping configurations and the coordinate system

Experiment

Experiments were conducted in the NIST laser Doppler velocimetry equipped Fluid Metering Research Facility. The flow facility has 5.25 cm (2.07 in) diameter, smooth, stainless steel piping, and the fluid is water. The source of flow is an NIST fluid metering calibration facility which uses an accurate weigh-time system to determine the bulk flow rate. However, during the tests the bulk flow rate is determined by using transfer standards. A magnetic flowmeter calibrated by the accurate weigh-time system is used to determine the test flowrate. This facility has a centrifugal pump to provide flow up to a diametral Reynolds number, $Re = W_b D / \nu$, exceeding 10^5 , where W_b is the bulk flow velocity, D is the inner pipe diameter and ν is the fluid kinematic viscosity. Water temperature is controlled using a heat exchanger to maintain a set temperature of 21°C. The relative roughness of this pipe has been measured with a profilometer to indicate a value of 0.006% based on interior pipe diameter. The pertinent parameters considered important in the current experiments are Reynolds numbers and pipe relative roughness; it is assumed that the fluid compressibility and gravitational effects are negligible.

The LDV system is described elsewhere.⁷ Briefly, it consists of a stationary, 2 W argon ion laser with dual beam optics mounted on a computer-controlled, six axes traversing system. Pertinent signal processing equipment produces appropriate computations. This system allows continuous movement of the measuring volume along each of the three perpendicular coordinate axes with a resolution of 5 μm . A thin-walled round glass pipe is used in the test section, which contains a water-filled enclosure having flat, thick (1.9 cm) optical glass sides, so that the laser beams are minimally deflected by the curvature of the round glass pipe. The LDV system is equipped with a Bragg-cell frequency shifter and so is capable of measuring low mean velocities with flow reversals. In this work, the dual-beam forward-scatter mode was adopted and counter signal processors have been used.

The pipeflows reported here are produced in smooth, stainless steel piping. The joints are arranged through weld-neck type flanges where special attention has been paid to smooth concentric alignments for all welded joints. All flange joints are concentrically aligned via pins; these joints are sealed using O-rings

to minimize gaps. Where steel pipe joins the glass tube test section, care was taken to produce a concentric joint with no abrupt changes in the inner pipe diameter.

Figure 1 is a sketch of the piping configurations and the coordinate system. The reducer used is of the standard belled (not conical) shaped type, and weld-neck flanges are welded onto both ends of the reducer configuration. This unit reduces the diameter from 7.79 cm (3.07 in) to 5.25 cm (2.07 in). The coordinate origin is chosen as the centre of the pipe in the exit plane of the reducer. The Z-coordinate is streamwise, with downstream being positive; X is the horizontal diameter and Y is the vertical coordinate with upwards being positive. The reducer installation was arranged so that over 100 pipe diameters (100D) of straight, constant diameter (7.79cm) piping preceded the reducer. A special radial inlet flow conditioner was installed at the upstream end of this length of piping so that no axial vorticity was produced by this entrance condition. Although the pipeflow produced by this inlet pipe has not as yet been directly measured, all previous LDV measurements downstream from the single elbow showed that the effects of the elbow were negligible after about 30 pipe diameters for Reynolds number 100 000 and relative roughness 0.006%. Since, in this 7.79cm (3.06in) diameter pipe, the Reynolds number was 66 000 (corresponding to 100 000 in the 5.25 cm pipe), the pipeflow profile after 100 diameters of this piping and the same pipe roughness conditions was assumed to be fully developed.

The reference condition of the facility can be arranged downstream of an approximately 200 constant diameter (5.25 cm) straight pipe. The measurements made include profiles of both streamwise and vertical components of the mean and turbulence velocities. In this arrangement, it is found that the pipe flow is fully developed, and its mean streamwise velocity is described very closely by the modified logarithmic profile of the Bogue and Metzner profile.⁸

The velocity measurements of the vertical component V and axial component W were made at varying axial distances, Z downstream from the exit plane of the reducer. In all of the results that follow, non-dimensionalized quantities will be used. Lengths and velocities are normalized using the inside pipe diameter D and bulk-average velocity W_b , respectively. Meter performances are given via orifice discharge coefficients C_d for three beta ratios (0.363, 0.50 and 0.75).

Results and discussion

Pipe flow measurements

Results presented and discussed here are for a single flow rate at a diametral Reynolds number Re of 10^5 . The time-averaged velocity components, W/W_b and V/W_b , respectively, in the streamwise and vertical directions along the horizontal diameter (X/D) at four different axial locations (Z/D) are shown in Figure 2. The data are presented by the symbols. The solid curve on Figure 2(a), the W component, is the fully developed equilibrated pipeflow distribution put forth by Bogue and Metzner.⁸ This streamwise velocity profile is the modified logarithmic distribution which would occur after the flow passes through very long lengths of straight, smooth, constant diameter piping.

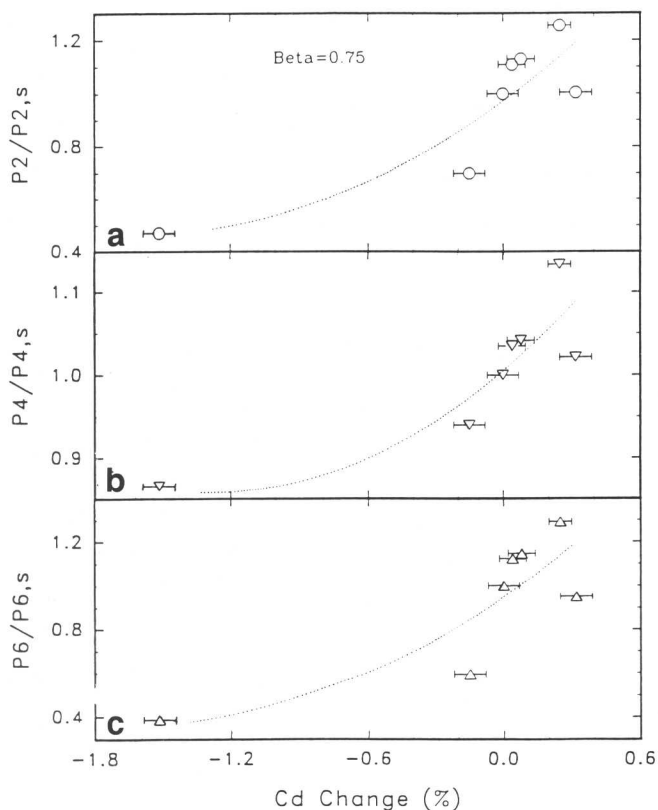


Figure 6 Relationship between the C_d change and profile peakness index for $\beta=0.75$: (a) P_2 , (b) P_4 and (c) P_6

obtained. Figures 6 and 7 show the relationships between C_d changes and the parameter indexes. Figure 6(a) shows the C_d change as a function of the peakness index $P_2/P_{2,s}$. The dotted line is a second-

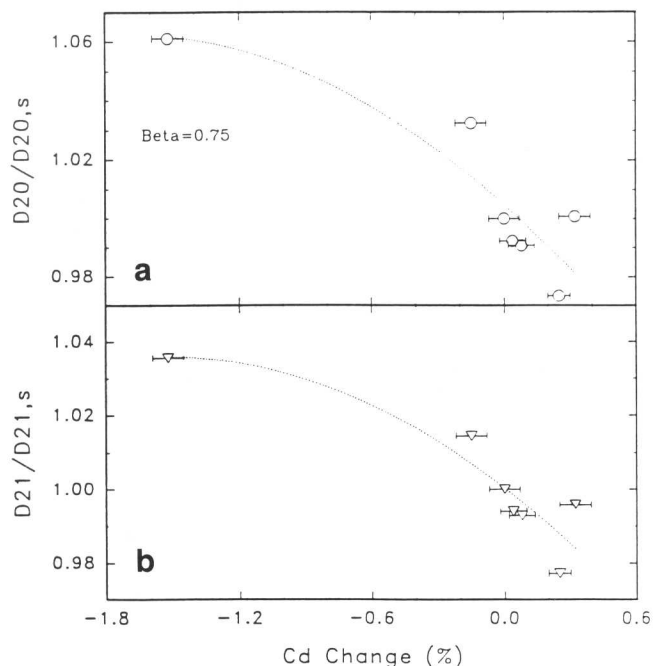


Figure 7 Relationship between the C_d change and flow displacement index for $\beta=0.75$: (a) D_{20} and (b) D_{21}

order regression curve fit. These data indicate there is a strong relationship between the peakness index P_2 and the C_d coefficient change. The relationship indicates that the C_d value in the non-ideal installation could be corrected somehow according to the empirical peakness- C_d curve.

Similar relationships for the peakness indexes $P_4/P_{4,s}$ and $P_6/P_{6,s}$ are presented in Figures 6(b) and (c), respectively. All these data show a quantitatively consistent relationship that a larger peakness produces a larger C_d coefficient. The prediction curves for the displacement indexes $D_{20}/D_{20,s}$ and $D_{21}/D_{21,s}$ are given in Figures 7(a) and (b), respectively. The data again show a strong relationship between the flow displacement indexes and the C_d change. Here, as expected, a larger displacement produces a smaller C_d coefficient.

These data show that all of the parameter indexes have a strong relationship with the meter performance. As expected, a profile having a smaller peakness or having larger displacement will result in a lower value of C_d or a negative C_d shift. This is due to the increased pressure drop across the orifice plate required to move the additional fluid near the wall through the hole in the orifice plate. As the profile peakness increases or the flow displacement decreases, the discharge coefficient C_d increases. All these curves indicate that the discharge coefficient C_d for the axisymmetric non-ideal installation conditions could be corrected through the empirical correlation curves. For these curves the P_4 and D_{21} parameters seem to have good prospects for making this compensation.

Summary and conclusions

Experimental measurements have been made using laser Doppler velocimetry and meter calibrations using gravimetric standards in the pipe flows produced by a reducer. This arrangement is known to be the cause of metering inaccuracies for meters installed in the downstream piping near these reducers. With a limited set of measurements of fluid velocity, the profile characteristics of the mean velocity downstream of a reducer is described both qualitatively and quantitatively. The flow is found to have profile characteristics that can strongly affect the performance of orifice flowmeters.

The velocity profile measurements made downstream from this reducer for the selected fluid indicate that the reducer initially produces a velocity profile that is flatter than the fully developed distribution that is pertinent to the Reynolds number and relative roughness conditions. With increasing downstream distance the pipeflow evolves from the flatter profile to a more peaked profile and then converses it to the fully developed pipeflow profile. The dissipation of the reducer effects does not occur with a monotonic progression of the mean axial velocity profile to that for the ideal distribution. Instead, the profile overshoots the ideal distribution to produce a core of fast flow in the centre of the pipeflow. Further downstream of the reducer the profile returns to the fully developed pipeflow.

Meters such as orifice plates, which can be sensitive to such profile anomalies, can be expected to show such effects. Three β ratio orifice meters were tested.

To quantify the peakness of the velocity profiles produced by the reducer, a range of peakness parameters are introduced. These include:

$$P_1 = \frac{W_c}{W_b} - 1 \tag{1}$$

$$P_2 = \frac{W_c^2}{W_b^2} - 1 \tag{2}$$

$$P_3 = 1 - \frac{W_b}{W_c} \tag{3}$$

$$P_4 = \frac{W_c}{W_w} \tag{4}$$

$$P_5 = \frac{\int (W_c - W) dr}{W_b D} \tag{5}$$

$$P_6 = \frac{\int (W_c^2 - W^2) dr}{W_b^2 D} \tag{6}$$

$$P_7 = \frac{\int W(W_c - W) dr}{W_b^2 D} \tag{7}$$

where W_c and W_w are the velocities at the pipe centreline and at a point near the wall ($r=0.475D$) respectively. All the parameters have a similar meaning for characterizing the distribution of the velocity field. A larger peakness index will mean high flow velocities, i.e. a more peaked profile near the centre core. Both P_1 and P_3 show the overshoot of the centreline velocity from the average bulk velocity, except that P_1 is normalized by the averaged bulk velocity while P_3 is normalized by the centreline velocity. P_2 is the overshoot of the centreline dynamic pressure over the dynamic pressure based on the averaged velocity. P_4 is the ratio between the centreline velocity and the velocity near the pipe wall (at 2.5% diameter from the wall). The parameters P_1 , P_2 and P_3 are determined only by the centreline velocity, P_4 is determined by two local velocities (the centreline and near-wall velocities), and P_5 , P_6 and P_7 are determined from the integration of velocities over the pipe diameter. These integrated quantities are similar to the displacement thickness and momentum thickness parameters commonly used in studying boundary layer flows.¹⁰

Other investigators have introduced some of these parameters in their studies. Klein^{11,12} called P_3 the block factor in studying the turbulent developing pipe flow and the effects of inlet conditions on conical diffuser performance. In studying the effect of flow profiles on orifice meter performance Ghazi¹³ has introduced the parameters F_1 and F_2 which are closely related to the peakness parameters P_1 and P_4 respectively: $F_1=1-P_3$ and $F_2=1/P_4$.

Besides these peakness parameters, other parameters that quantify how the flow is displaced from the centre of the pipe can also be used. A more peaked flow at the pipe centre will mean that the flow is more concentrated here and less displaced from the pipe centreline. A displacement parameter is thus introduced to quantify the average flow displacement from the pipe centreline for a selected quantity, as follows:

$$D_{mn} = \frac{\int r W^m r^n dr}{D \int W^m r^n dr} \tag{8}$$

Here four flow displacement parameters are considered. D_{10} is for the velocity W , D_{11} is for the first radial moment of axial velocity, Wr , D_{20} is for the dynamic pressure W^2 , and D_{21} is for the first radial moment of the dynamic pressure, W^2r .

These profile peaknesses and flow displacements as functions of the axial distance downstream from the reducer for $Re=100\,000$ are shown in Figure 5. To compare these with the values for the fully developed profile these parameters are normalized by those of the straight pipe case, denoted with a subscript, s. Thus, if a profile is flatter than the ideal profile, the value of the peakness will be less than one. In this case, the flow field is displaced further from the centre line and the value of this displacement should be larger than 1.

Figures 5(a) and (b) show the peakness indexes, $P_i/P_{i,s}$ as functions of Z/D , while Figure 5(c) is for the displacement indexes, $D_{mn}/D_{mn,s}$ as functions of Z/D . As shown in Figure 5, at small values of Z/D the peaknesses are less than one. With downstream distance, the values increase to and through 1 to reach respective maximal values and then decrease monotonically to the ideal case of 1. The sequence is opposite for the flow displacement parameters. As shown in Figure 5(c), the displacement indexes are greater than one for small values of the distance Z/D . With downstream distance, they decrease and pass the value of 1 to reach respective minima, and then approach monotonically the ideal value of 1.

Now that we have the distribution data for both orifice meter performance and the flow profile indexes we can analyse the correlations between them. From Figure 4(b) and Figure 5 the relationship can be

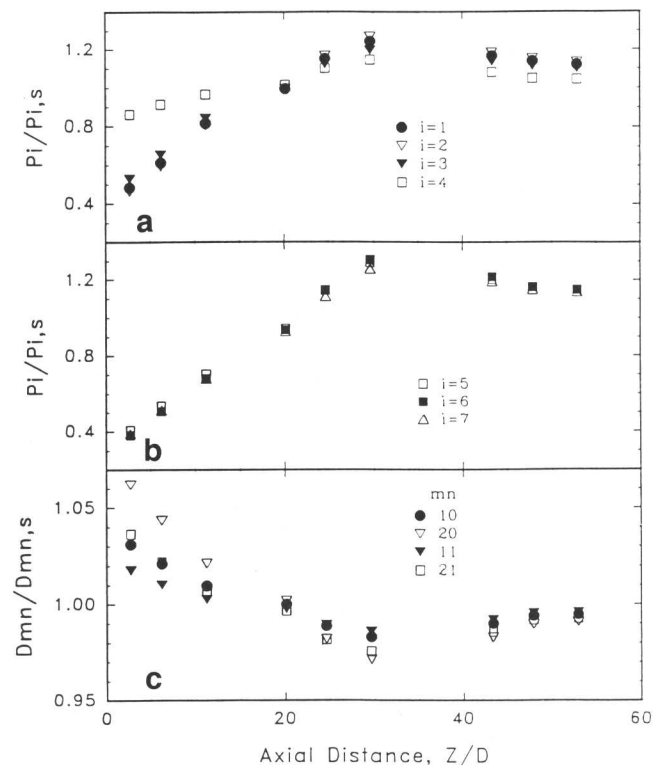


Figure 5 Profile indexes downstream of a reducer for $Re=100\,000$. (a) and (b) are for peakness and (c) is for displacement

Orifice meter downstream of the reducer

Figure 4 presents results for orifice meters downstream of the reducer shown in Figure 1. The ordinate in each of these figures is the percentage shift in discharge coefficient (C_d) relative to that obtained for the reference condition at each flowrate. Figure 4(a) shows the C_d change versus pipe Reynolds number Re for $\beta=0.75$ and four different installation positions. The symbols plotted are the data, and the curves are the third-order least square fits to the data. At each flow rate, five data points are obtained. The results for $\beta=0.363$ and 0.50 are similar and are not shown here. These results show that for all β ratios the discharge coefficient is shifted negatively when the orifice meter is installed near the reducer. As the distance between the orifice meter and the reducer increases, the negative C_d shift decreases. This decrease continues until a 'zero-shift' installation location occurs. For installations beyond this location the shift overshoots the zero shift condition, becomes positive, reaches a maximum and then returns to zero about 50–60 diameters downstream from the reducer.

Figure 4(b) presents the results in a different format. In this figure the results obtained for the different meter geometries tested downstream of this reducer are presented. Again, the ordinate is the percentage change in discharge coefficient relative to the reference value at each flow rate. In this case, the abscissa is the downstream distance from the reducer. Only three test conditions are shown. In each case the data are for the highest Reynolds number tested for each β ratio.

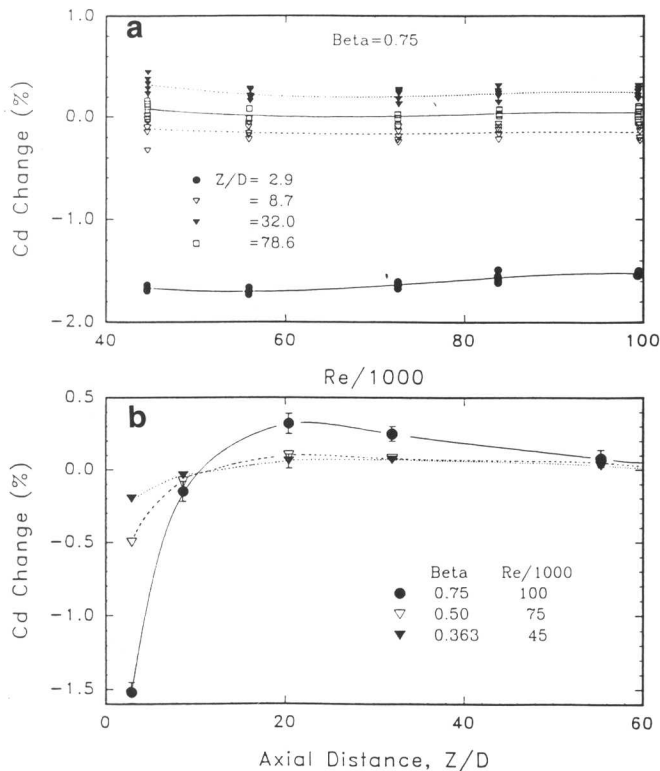


Figure 4 Percentage change in discharge coefficient (a) for a $\beta=0.75$ orifice meter vs. Re and (b) for three values of β as functions of the distance downstream of a reducer for $Re=100\ 000$. (a) and (b) are for peakness and (c) is for displacement

The data are shown by the symbols and each data point is an average of five determinations, as are those shown in Figure 4(a). The curves are cubic spline fits to the averaged data. The error bars denote one standard deviation of the repeated readings about the mean value.

These results show clearly the dependence of the orifice characteristics for the three meters at the same meter locations. The shifted discharge coefficients are considered sizeable, especially for larger β ratio meters. The amount of negative shift ranges from about -0.2% for the small β of 0.363 to -1.6% for the largest β of 0.75 . For installations near the reducer, at $Z/D=2.9$, where all of the discharge coefficients are shifted negatively with respect to the reference values, the $\beta=0.75$ meter has a deviation that is about eight times that for the $\beta=0.363$ meter.

When the orifice meter is installed further from the reducer, these negative shifts diminish and become zero at around a downstream position of $11\text{--}13D$ from the reducer. However, with increased downstream distance, orifice discharge coefficients are shifted positively relative to reference values. These positive shifts appear, from these results, to be maxima at the installation position $20D$ downstream from the reducer. These maxima also appear to be dependent upon the β ratio, with the smallest shift of about $+0.1\%$ occurring for $\beta=0.363$ at the $30D$ location and the largest of about $+0.3\%$ for $\beta=0.75$ at the $20D$ location. For practical purposes, there is no overshoot situation for the cases of $\beta=0.50$ and 0.363 ratio, and beyond $Z/D=10$ the shift can be considered essentially zero, since these positive overshoots are less than 0.1% .

As for the largest β ratio of 0.75 , when the installation is made further than $20D$ downstream of the reducer, the results show that the positive shifts in discharge coefficient decrease, so that deviations from reference condition values are essentially less than 0.1% beyond the $55D$ location.

Profile peakness and flow displacement

The results previously presented include both the velocity profiles and the meter performance downstream of the reducer. The next effort is to seek the relationship between the two and to find some criteria for improving the meter performance prediction in these non-ideal conditions.

Different piping configurations produce different velocity profiles. These different velocity profiles could significantly affect flowmeter performance. Based on the measured velocities, various flow field parameters can be defined and quantified. Some parameters may be more important than others in affecting meter performance. Previous research results have shown that swirling flows produced by several different pipe configurations can have very strong effects on the meter performance of selected meters.^{1,5}

One quantity believed to be important in the performance of orifice meters is the character of the peakness or the flatness of the velocity profile. Because the velocity field produced by the reducer is a swirl-free, skew-free, axisymmetric flow, as shown earlier, this flow field is a good candidate for studying the effects of profile peakness on orifice meter performance.

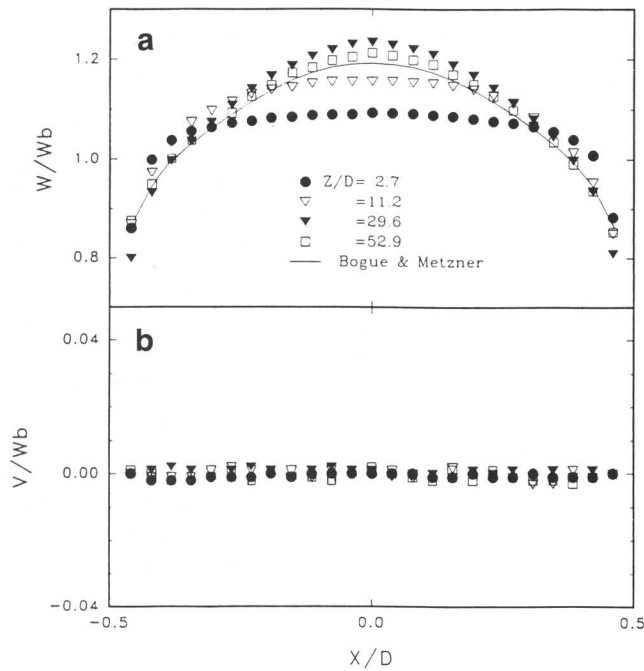


Figure 2 Mean velocity profiles of the streamwise and vertical components downstream of a reducer vs. the horizontal diameter positions for $Re=100\ 000$. The solid line is the ideal pipe flow of Bogue and Metzner⁸

The effects of the reducer produce, near the exit of the reducer ($Z/D=2.7$), very uniform velocity profiles compared with the fully developed distributions for these conditions as indicated in Figure 2(a). With downstream distance, the mean velocity profile approaches the fully developed pipeflow. At $Z/D=11.2$, the streamwise velocity profile continues to show that the centre core of this flow is slower and the flow in the wall region is higher than the corresponding fully developed velocities. The diameter of this slow core region is about one third of the pipe diameter. However, at the $20D$ location, the profile shows that the centre core of this pipeflow crosses over and produces velocities in excess of the fully developed distribution in the centre portion of the pipeflow. The crossover position where the profile closely approximates the fully developed pipeflow distribution is about $20D$ downstream of the exit of the reducer. The diameter of this fast flow core is about one-half of a pipe diameter; the maximum velocity measured in these results is about 5% greater than the centreline value for the fully developed distribution. This fast core flow continues to grow as indicated at $Z/D=29.6$ and then decreases to that of the fully developed flow profile as the distance increases.

Figure 2(b) shows the vertical mean velocity profiles V/W_b versus horizontal radial position at different downstream positions from the reducer for $Re = 100\ 000$. These results show that the reducer does not appear to produce transverse velocity or swirl flow. For an ideal fully developed pipeflow these velocities should be zero everywhere.

The root mean square (r.m.s.) turbulent velocity profiles of the axial (w'/W_b) and vertical (v'/W_b) components downstream of the reducer at four axial locations

(Z/D) are presented in Figure 3. Figures 3(a) and (b) are the profiles along the horizontal radial position from the pipe-centreline, while in Figure 3(c) the radial position is along the vertical y -axis. For comparison, the results measured by Laufer at $Re=41\ 000$ ⁹ are also shown in the figure via the solid profile. These results indicate that the turbulent intensity near the exit of the reducer in the centre core of the pipe is lower than the result given by Laufer. Near the pipe walls, the intensity exceeds the levels measured by Laufer. The lower turbulent intensity in the centre core of the pipe is due to the fact that the turbulence found in the fully developed flow upstream of the reducer in the 7.79 cm pipe is convected through the reducer without significant change and is normalized with the higher bulk average velocity in the smaller 5.25 cm pipe. With downstream distance, the turbulent velocity increases and approaches the new fully developed pipeflow in the 5.25 cm diameter pipe. At $Z/D=29.6$, the streamwise turbulent velocity is very close to the Laufer data. However, the vertical component of the turbulent velocity is still lower than those of Laufer even at $Z/D=52.9$, especially near the centre core.

The velocity profiles shown are presented along the horizontal diameter, since the data indicate that these pipeflows are essentially axisymmetric at all stations measured.

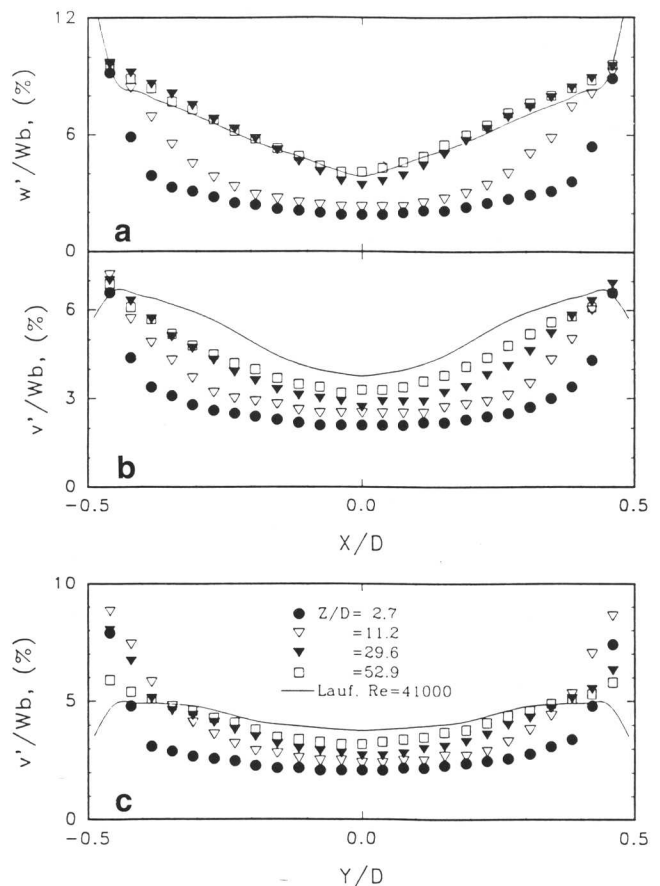


Figure 3 Root mean square turbulent velocity profiles of the streamwise and vertical components downstream of a reducer for $Re=100\ 000$. (a) w'/W_b vs. X/D , (b) v'/W_b vs. X/D and (c) v'/W_b vs. Y/D . Solid lines refer to Laufer's data⁹ at $Re=41\ 000$

Results show that there is a pronounced β ratio dependence in the orifice characteristics. Low β ratios (~ 0.36) are hardly affected except where they are installed close to the reducer; large ratios (0.75) show significant deviations from ideal discharge coefficient values, and they show strong dependence upon profile overshoot.

It is now well known that the different velocity profiles produced by different pipe configurations can significantly affect flowmeter performance. These include swirl, skew and turbulence. The effects of the profile peakness on orifice meter performance are the focus of the present experimental study. Several profile indexes are introduced to characterize the profile peaknesses and flow displacements. These indexes are then correlated with orifice meter performance. It is shown that these profile indexes have strong relationships with the changes in the discharge coefficient of the different orifice meters and thus could be used to develop criteria for improving the meter performance in axisymmetric non-ideal installation conditions.

Acknowledgements

The authors acknowledge the partial support of the industry–government consortium formed at NIST to investigate pipeflow fluid mechanics and corresponding meter performance under non-ideal installations. Special acknowledgement is made for the support provided by the Gas Research Institute, Chicago IL.

References

- 1 **Mattingly, G. E. and Yeh, T. T.** NIST's industry–government consortium research program on flowmeter installation effects: Report of results for the research period July–December 1987, *NISTIR-88-3898*, November 1988
- 2 **Mattingly, G. E. and Yeh, T. T.** NIST's industry–government consortium research program on flowmeter installation effects: Report of results for the research period January–July 1988, *NISTIR-89-4080*, April 1989
- 3 **Mattingly, G. E. and Yeh, T. T.** NIST's industry–government consortium research program on flowmeter installation effects: Report of results for the research period November 1988–May 1989, *NISTIR 4310*, April 1990
- 4 **Mattingly, G. E. and Yeh, T. T.** Effects of non-ideal pipeflows and tube bundles on orifice and turbine meters, *Flow Meas. Instrum.* (1991) **2** 1–19
- 5 **Mattingly, G. E. and Yeh, T. T.** Flowmeter installation effects, *Proc. National Conference of Standards Laboratories Annual Conference*, Washington DC, August 14–18, 1988, NCSL, Boulder CO.
- 6 **ASME, MFC-10M** Method for establishing installation effects on flowmeter, *Am. Soc. Mech. Eng.* November 1988, New York, NY 10017.
- 7 **Yeh, T. T., Robertson, B. and Mattar, W. M.** LDV measurements near a vortex shedding strut mounted in a pipe, *J. Fluids Eng.* **ASME**, **105** (1983) 185–196
- 8 **Bogue, D. C. and Metzner, A. B.** Velocity profiles in turbulent pipe flow, *I&EC Fundamentals*, **2** (2) (1963) 143–149
- 9 **Laufer, J.** The structure of turbulence in fully developed pipe flow, *NBS Rept 1974*, September 1952
- 10 **Schlichting, H.** 'Boundary Layer Theory', 4th edn, McGraw-Hill, New York (1960)
- 11 **Klein, A.** Review: Turbulent developing pipe flow, *J Fluids Eng.* **103** (1981) 243–249
- 12 **Klein, A.** Review: Effects of inlet conditions on conical-diffuser performance, *J. Fluids Eng.* **103** (1981) 250
- 13 **Ghazi, H. S.** A pressure index for predicting the effect of flow profiles on orifice meter performance, *J. Basic Eng.* March (1966) 93–100